Electronic Supplementary Material (ESI) for Journal of Materials Chemistry C.

A Tough, Anti-freezing, and Low-dehydration Rate Gelatin Hydrogel with Inverse Temperature-dependent Ionic Conductivity

Aiman Saeed[a], Syed Farrukh Alam Zaidi[b*], Junyoung Mun[c], Hyung Koun Cho[c,d], Seung-Boo Jung[c,d], Nae-Eung Lee[c,d,e], Chun Gwon Park[a,e*], Jung Heon Lee[c,d,e,f *]

[a] Department of Biomedical Engineering, Sungkyunkwan University, Suwon 16419, Republic of Korea

[b] Department of Metallurgical and Materials Engineering, University of Engineering and Technology (UET), Lahore, 39161, Pakistan

[c] School of Advanced Materials Science and Engineering, Sungkyunkwan University (SKKU), Suwon 16419, Republic of Korea

[d] Research Center for Advanced Materials Technology, Core Research Institute, Suwon 16419, Republic of Korea

[e] Biomedical Institute for Convergence at SKKU (BICS), Sungkyunkwan University (SKKU), Suwon 16419, Republic of Korea

[f] Department of MetaBioHealth, Sungkyunkwan University (SKKU), Suwon, 16419 Republic of Korea

***Corresponding Authors:** farrukhzaidi@uet.edu.pk (Syed Farrukh Alam Zaidi); chunpark@skku.edu (Chun Gwon Park); jhlee7@skku.edu (Jung Heon Lee)

S1. Evaluation of Strain-sensing cability of hydrogels

To demonstrate the strain-sensing capability of the hydrogel, a simple electric circuit was constructed comprising a blue LED, a battery, and a hydrogel sample. The hydrogel acted as a resistive component in this setup. As the hydrogel was subjected to varying degrees of strain by stretching and releasing, the subsequent relative change in resistance was determined using a Digital Multimeter (DT9205A). The strain-sensing performance was then graphically represented by plotting the relative resistance change ($\Delta R/R_o$) against the applied strain (ε). The gauge factor (GF) was derived from this relationship using equation S1.

$$GF = \frac{\Delta R / R_o}{\varepsilon} = \frac{(R - R_o)/R_o}{\varepsilon} \qquad (S1)$$

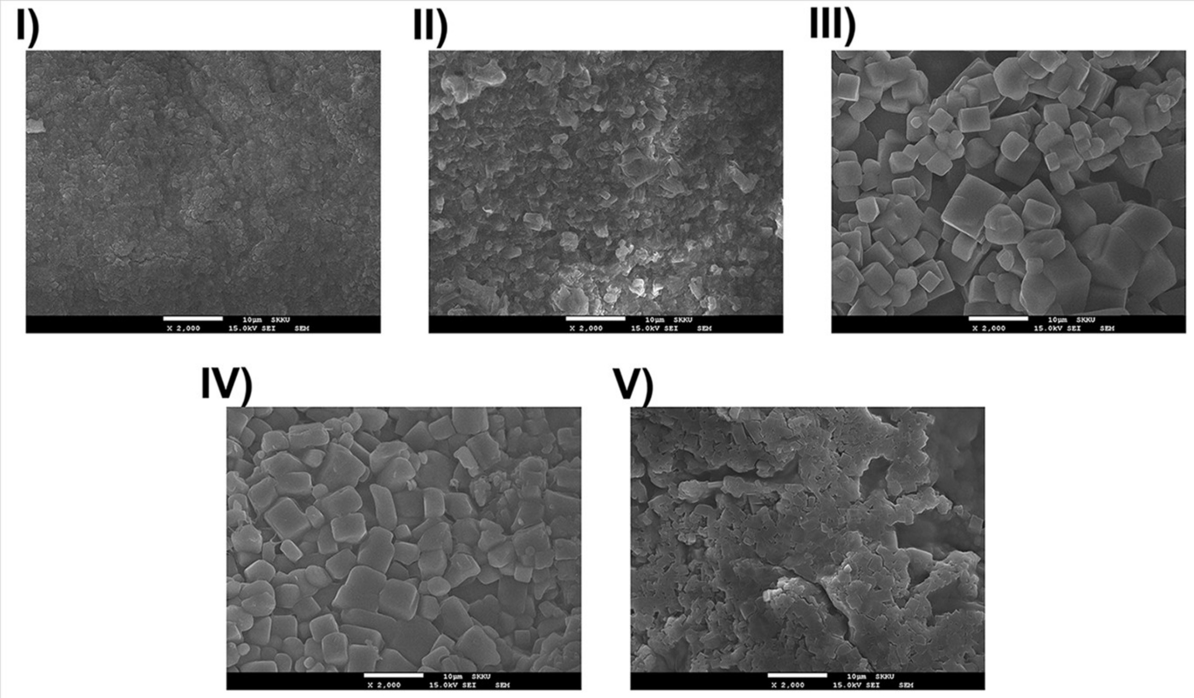

Fig. S1 Microstructure analysis, using SEM, of hydrogels prepared in various wt% ratio of the AmAc and AmC containing composite salt solution.

Fig. S2 Load lifting capability of $[Gel_{10}](AmAc_{55}AmC_5)$ hydrogels, indicating excellent mechanical toughness.

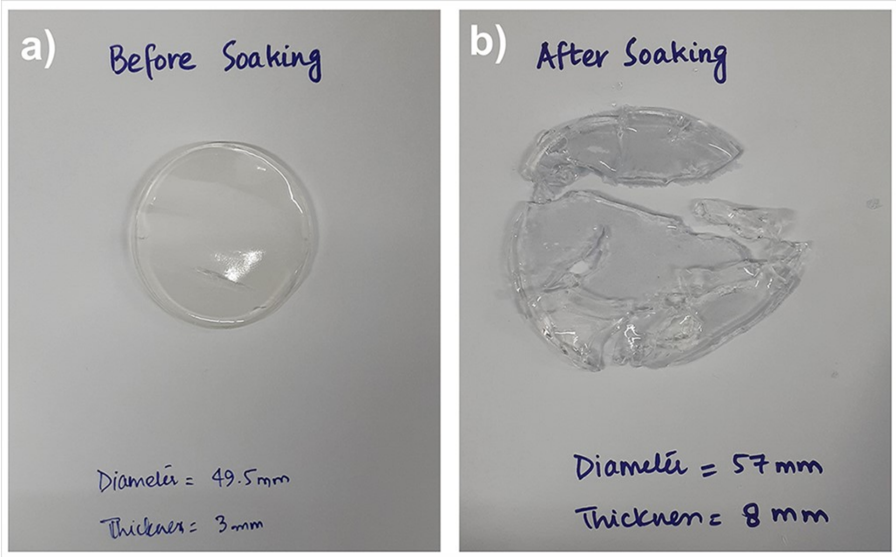

Fig. S3 Appearance of (a) $[Gel_{10}]$ hydrogel and (b) as prepared $[Gel_{10}](AmC_5)$ hydrogel.

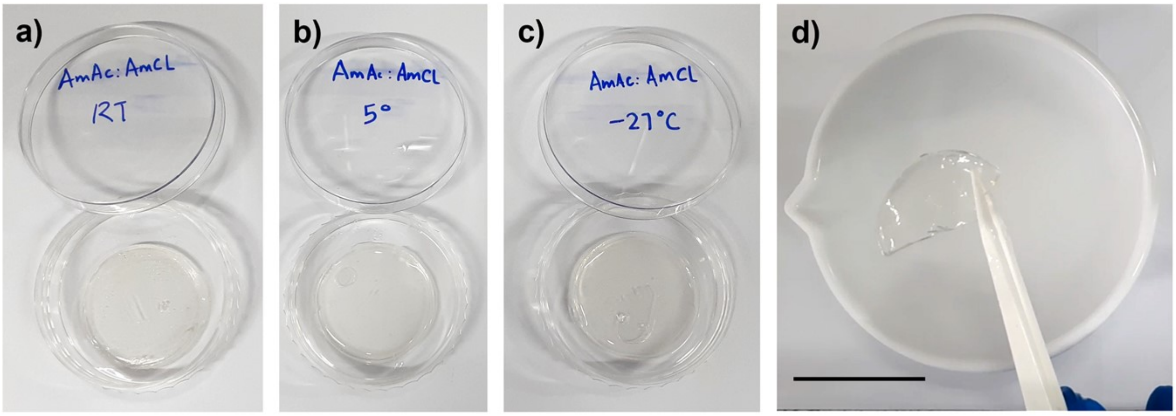

Fig. S4 Transparent appearance and no precipitation of salt particles in $[Gel_{10}](AmAc_{55}AmC_5)$ hydrogel at various temperatures: (a) room temperature (RT), (b) 5°C, (c) -27°C, and (d) liquid nitrogen.

Fig. S5 Precipitation of solids in hydrogels containing various wt% ratio of the AmAc and AmC salts.

The probable phenomena of the precipitation could be explained by considering that the hydrogel releases water from its structure when immersed in a salt solution, a process known as the "salting out" effect [S1,S2]. During this process, the components of the salts are absorbed into the hydrogel. In the present case, the mixture includes two salts, AmAc and AmC, each with distinct solubility in water. AmAc is notably more soluble in water than AmC. The anions from these salts, CH_3COO^- and Cl^-, could interact in such a way that influences their solubility. Upon cooling, it is probable that AmC, due to its lower solubility, precipitates out of the solution. This could be an example of the common ion effect in line with Le Chatelier's Principle.

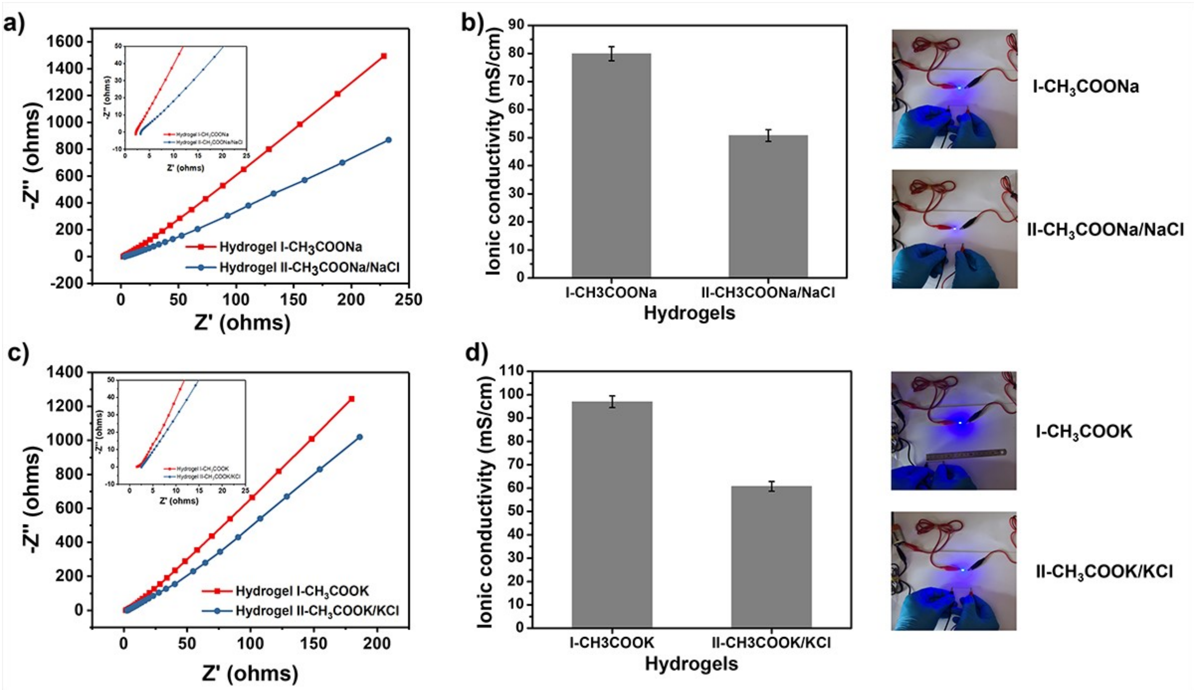

Fig. S6 (a,b) EIS data, ionic conductivity, and corresponding blue LED's brightness of Hydrogel I-CH_3COONa and Hydrogel II-CH_3COONa/NaCl and (c,d) EIS data, ionic conductivity, and corresponding blue LED's brightness of Hydrogel I-CH_3COOK and Hydrogel II-CH_3COOK/KCl at RT.

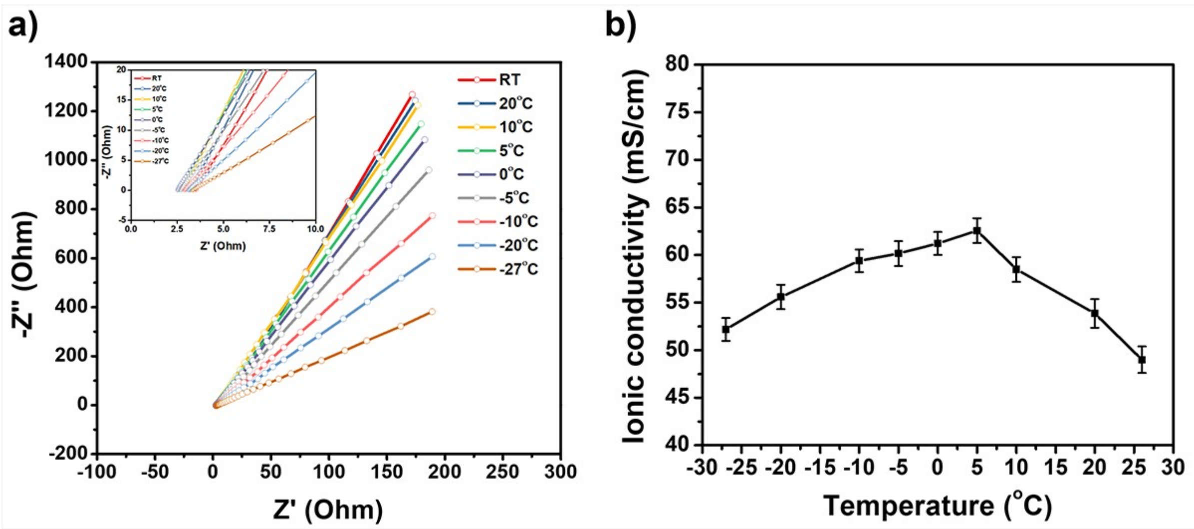

Fig. S7 (a) EIS data and (b) ionic conductivity of Hydrogel II across a detailed temperature range, RT, 20°C, 10°C, 5°C, 0°C, -5°C, -10°C, -20°C, and -27°C.

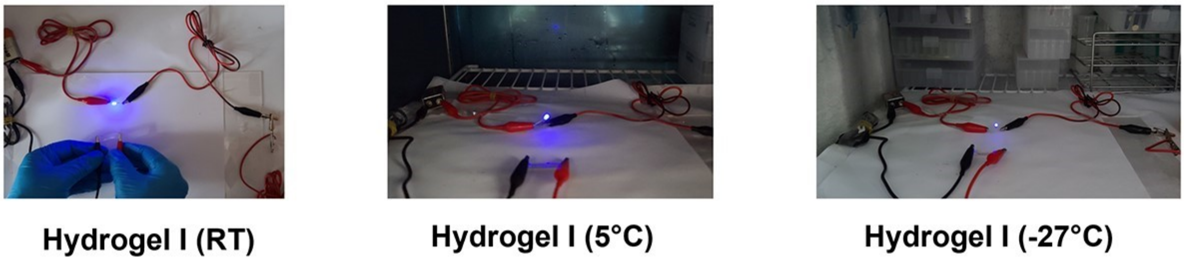

Fig. S8 Blue LED's brightness using the Hydrogel I as function of temperature.

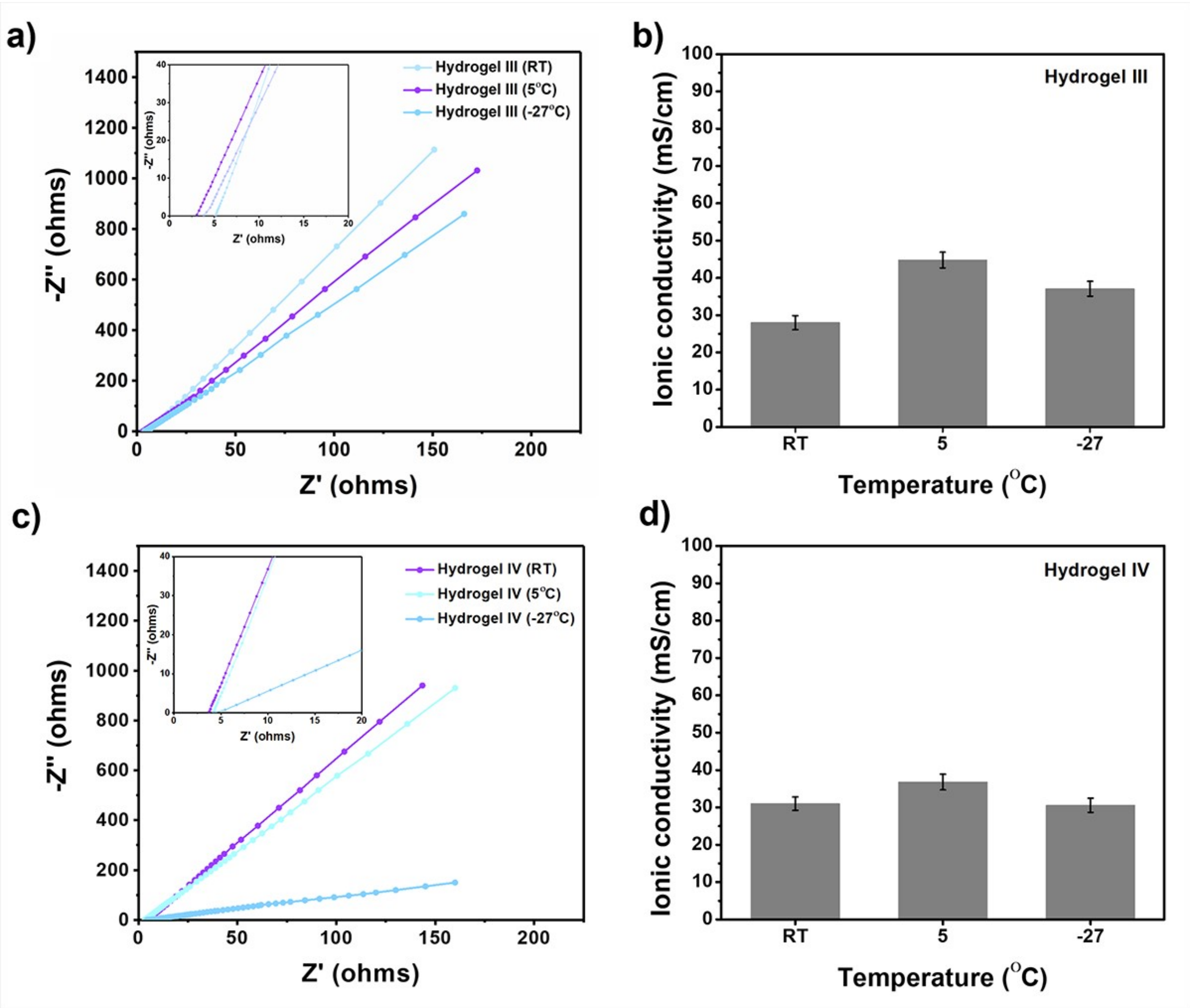

Fig. S9 (a) EIS curves and (b) ionic conductivity of Hydrogel III at different temperatures of RT, 5°C, and -27°C. (c) EIS curves and (d) ionic conductivity of Hydrogel IV at different temperatures of RT, 5°C, and -27°C.

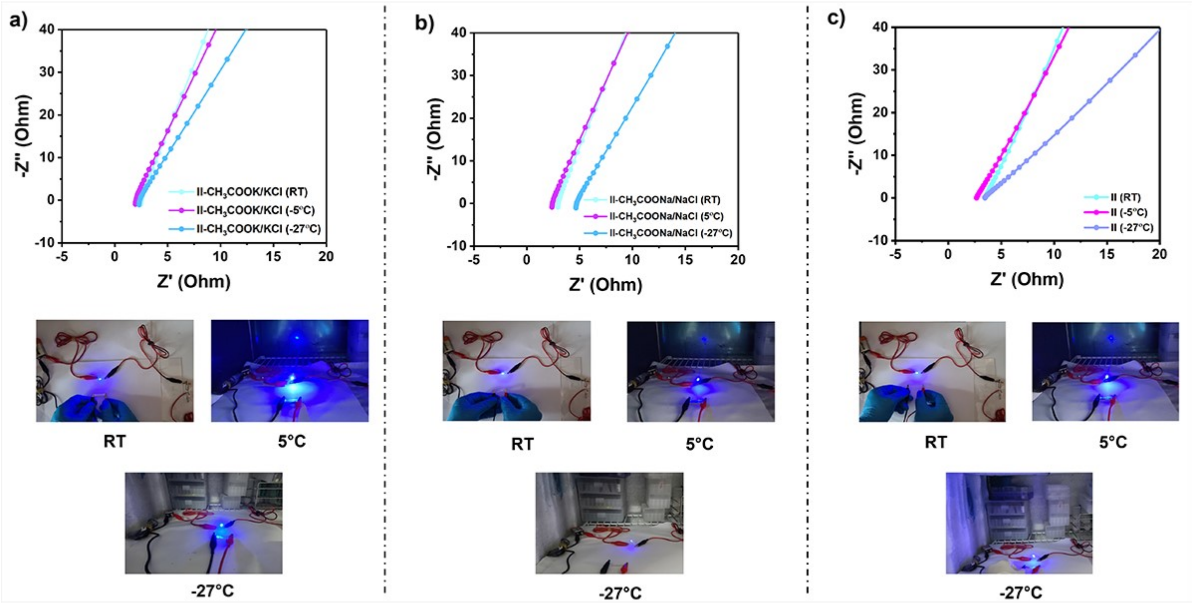

Fig. S10 EIS data and blue LED's brightness of the hydrogels II-CH_3COOK/KCl, II-CH_3COONa/NaCl and II at RT, 5°C and -27°C.

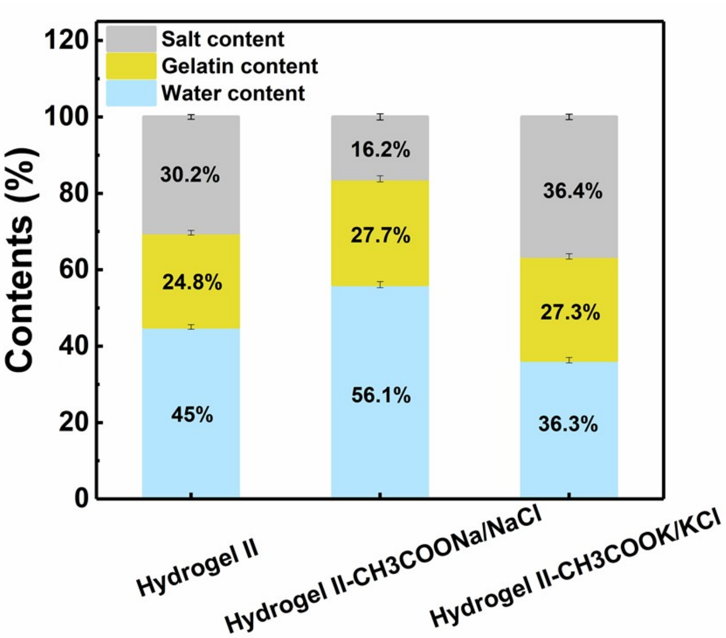

Fig. S11 Water and solid contents (gelatin and salt) of the Hydrogel II, Hydrogel II-CH_3COONa/NaCl and Hydrogel II-CH_3COOK/KCl.

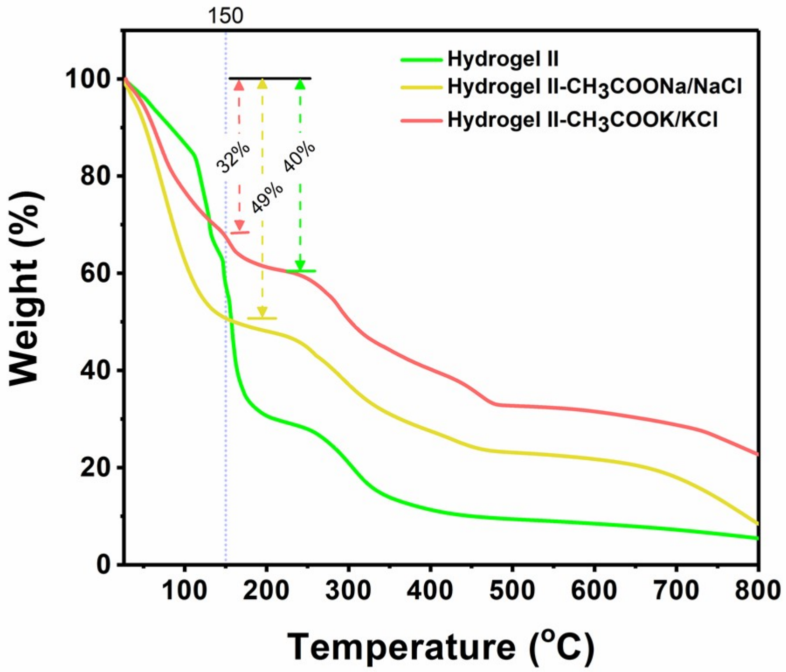

Fig. S12 Water and solid contents of the Hydrogel II, Hydrogel II-$CH_3COONa/NaCl$ and Hydrogel II-CH_3COOK/KCl using TGA within 150°C of the water removal range.

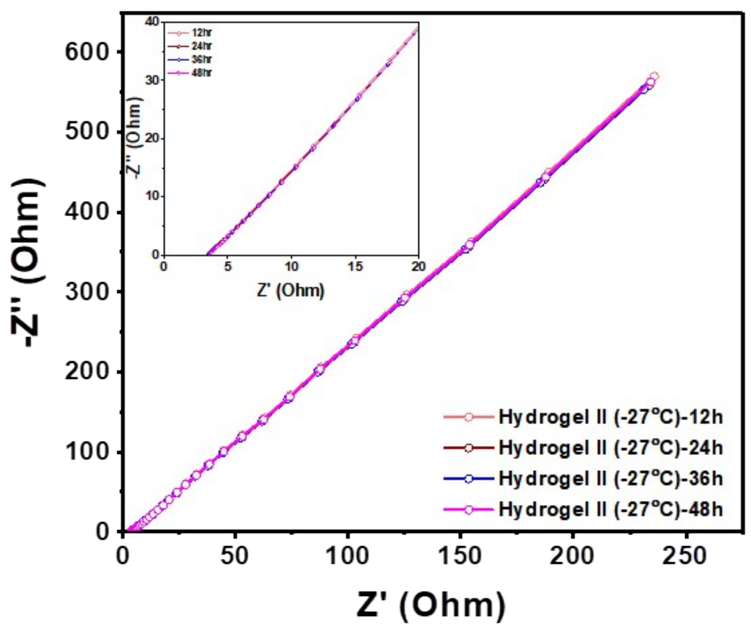

Fig. S13 EIS data of Hydrogel-II at -27°C for periods of 12h, 24h, 36h and 48h.

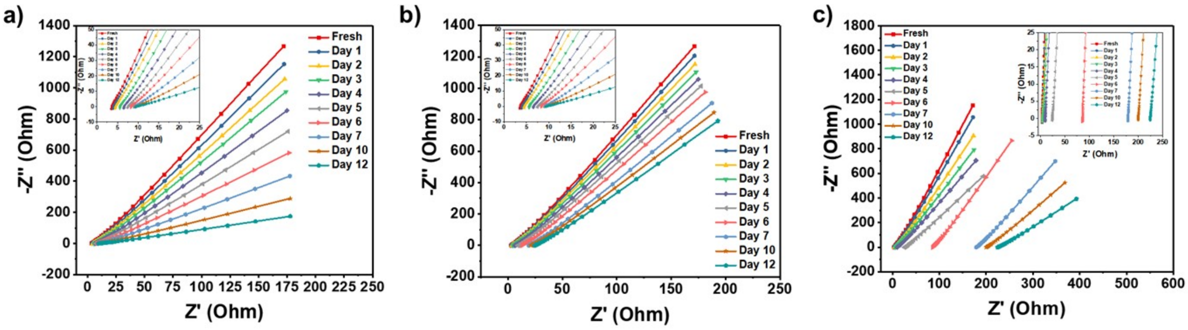

Fig. S14 EIS data of Hydrogel-II at (a) RT, (b) 5°C, and (c) -27°C during drying experiment.

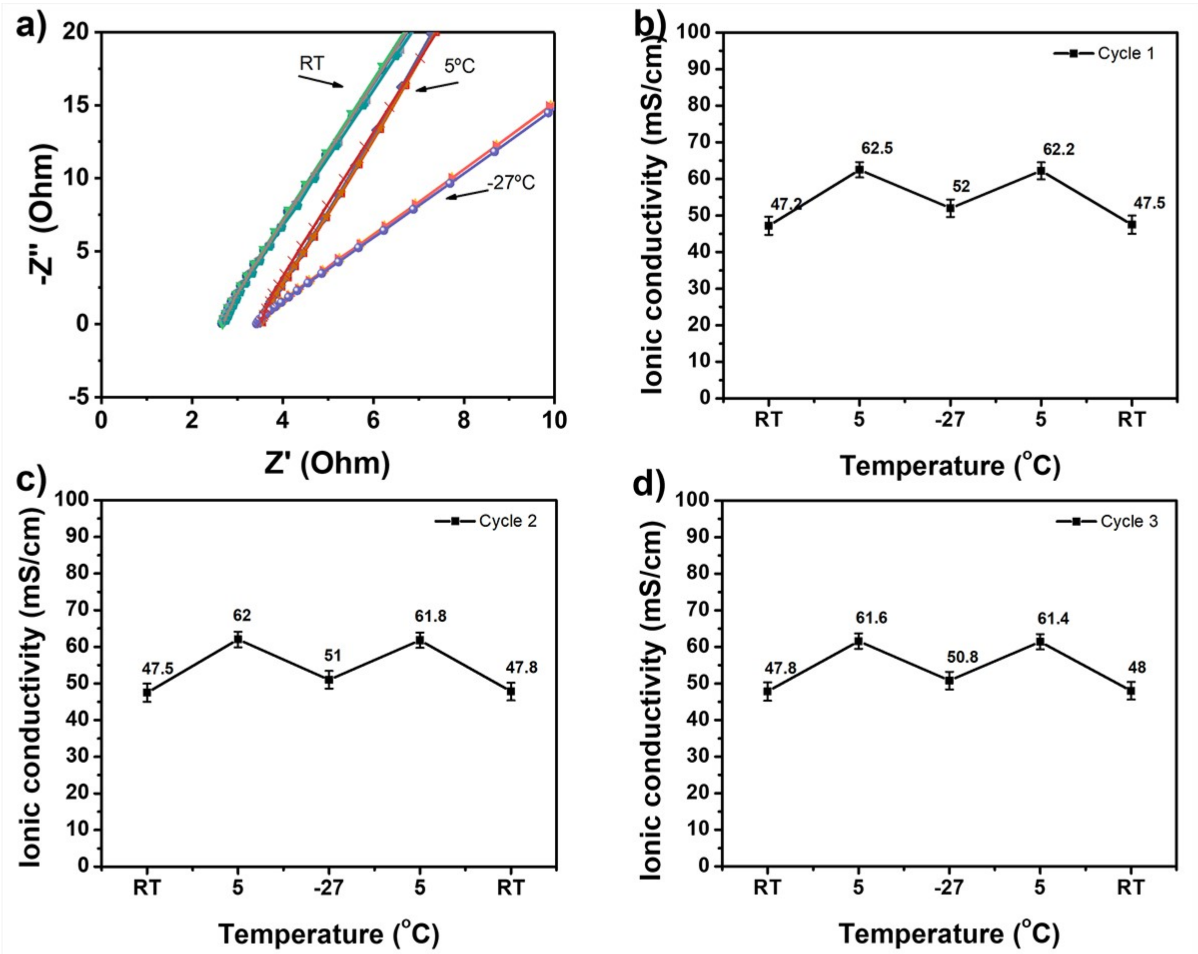

Fig. S15 Reversibility of electrochemical properties of Hydrogel II for three cycles of cooling and heating. (a) EIS data, and (b, c and d) ionic conductivity.

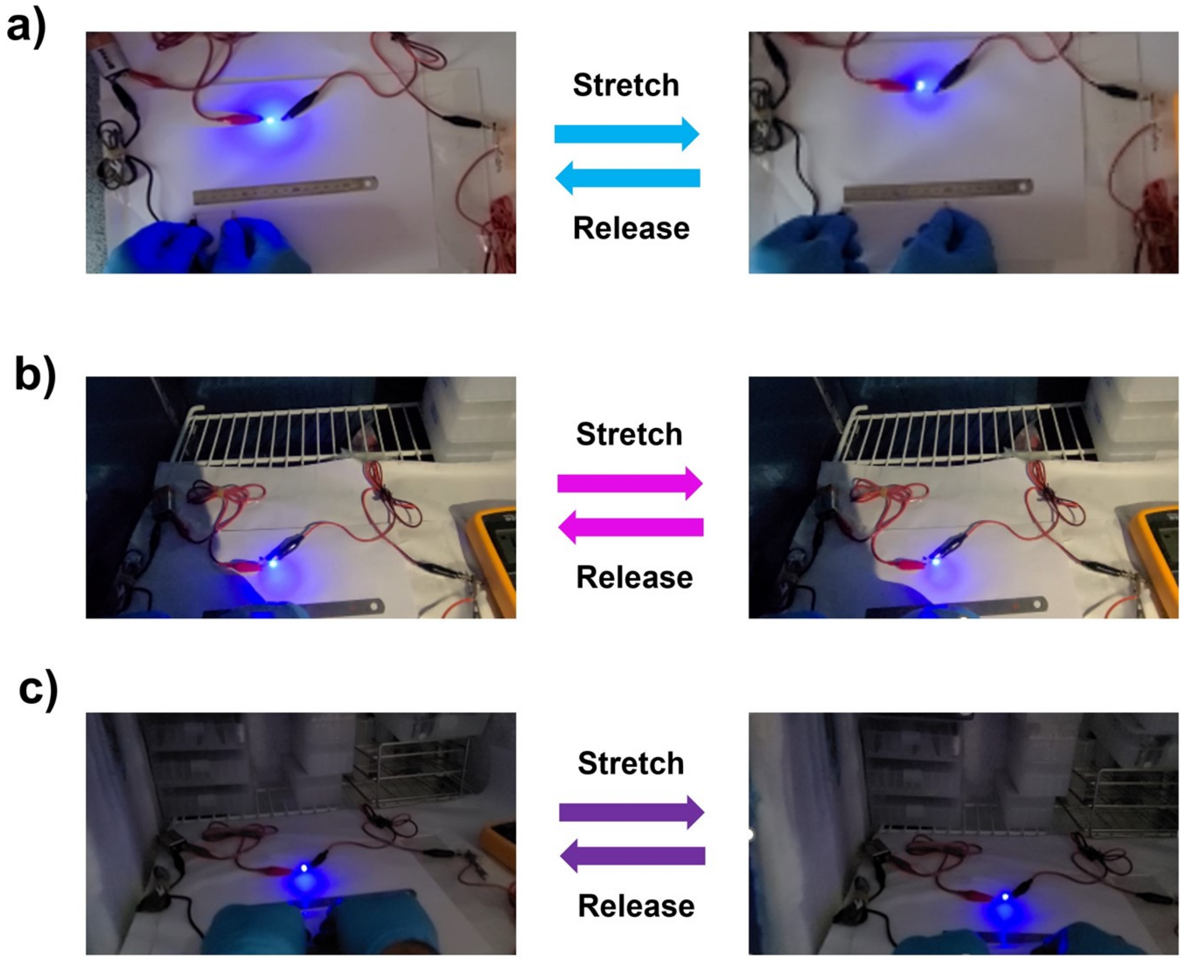

Fig. S16 Hydrogel II as resistive strain sensor: change in brightness of blue LED at (a) RT, (b) 5°C, and (c) -27 °C.

Table S1. Comparison of the mechanical and electrochemical performance of proposed hydrogels with that of the state-of-the-art anti-freezing and low dehydration rate hydrogels

Ref.	Hydrogel system	Mechanical toughness	Ionic conductivity at RT	Ionic conductivity at subzero	Comments
[S3]	poly (sulfobetaine-co-acrylic acid)/ LiCl	-	11 S/m	3 S/m at -20°C	Mechanical toughness is not mentioned; Tensile strength drops with higher LiCl content and ionic conductivity.
[S4]	PVA/malic acid/$CaCl_2$	-	5.3 S/m	-	No toughness data; tensile strength < 100 kPa. No subzero ionic conductivity was mentioned.
[S5]	PDMAPS/PDMAPS-*co*-PAA/$CaCl_2$	-	9 S/m	3.8 S/m at -50°C	No data on mechanical properties
[S6]	*κ*-CG-$CaCl_2$	-	-	-	Hydrogel used for dehydration and anti-icing; no ionic conductivity data. No focus on mechanical toughness (tensile strength < 50

					kPa).
[S7]	Gelatin/Na-citrate/glycerol	4 MJ/m^3	0.47 S/m	-	Limited ionic conductivity at RT due to presence of glycerol for freezing tolerance and dehydration resistance. Ionic conductivity at subzero temperature is not mentioned.
[S8]	Gelatin/Na-citrate/NaCl/glycerol	0.4 MJ/m^3	1.6 S/m	0.4 S/m at -20ºC	Limited ionic conductivity at RT due to presence of glycerol for freezing tolerance and dehydration resistance. Ionic conductivity at subzero temperature is not mentioned.
This work	Gelatin/NH_4acetate/NH_4Cl	1147 kJ/m^3 (1.147 MJ/m^3)	4.72 S/m	5.21 S/m at -27°C	High ionic conductivity at RT due to glycerol free hydrogel compositions with

					freezing tolerance and dehydration resistance. Increased ionic conductivity at subzero temperature.

[S1] X. Wang, C. Qiao, S. Jiang, L. Liu, J. Yao, Strengthening gelatin hydrogels using the Hofmeister effect, Soft Matter. 17 (2021) 1558–1565. https://doi.org/10.1039/D0SM01923B.

[S2] Q. He, Y. Huang, S. Wang, Q. He, Y. Huang, S. Wang, Hofmeister effect-assisted one step fabrication of ductile and strong gelatin hydrogels, Adv. Funct. Mater. 28 (2018) 1705069. https://doi.org/10.1002/ADFM.201705069.

[S3] X. Sui, H. Guo, C. Cai, Q. Li, C. Wen, X. Zhang, X. Wang, J. Yang, L. Zhang, Ionic conductive hydrogels with long-lasting antifreezing, water retention and self-regeneration abilities, Chem. Eng. J. 419 (2021) 129478. https://doi.org/10.1016/j.cej.2021.129478.

[S4] Q. Wang, X. Pan, H. Zhang, S. Cao, X. Ma, L. Huang, L. Chen, Y. Ni, Fruit-battery-inspired self-powered stretchable hydrogel-based ionic skin that works effectively in extreme environments, J. Mater. Chem. A. 9 (2021) 3968–3975. https://doi.org/10.1039/D0TA09149A.

[S5] Q. Shi, J. Mao, Y. Cai, H. Gao, S. Li, D. Cheng, Bioinspired ionic hydrogel materials with excellent antifouling properties and high conductivity in dry and cold environments, Polym. Chem. 13 (2022) 4711–4716. https://doi.org/10.1039/D2PY00750A.

[S6] T. Li, K. Xu, L. Shi, J. Wu, J. He, Z. Zhang, Dual-ionic hydrogels with ultralong anti-dehydration lifespan and superior anti-icing performance, Appl. Mater. Today. 26 (2022) 101367. https://doi.org/10.1016/J.APMT.2022.101367.

[S7] Z. Qin, X. Sun, H. Zhang, Q. Yu, X. Wang, S. He, F. Yao, J. Li, A transparent, ultrastretchable and fully recyclable gelatin organohydrogel based electronic sensor with broad operating temperature, J. Mater. Chem. A. 8 (2020) 4447–4456. https://doi.org/10.1039/C9TA13196E.

[S8] M. Wu, X. Wang, Y. Xia, Y. Zhu, S. Zhu, C. Jia, W. Guo, Q. Li, Z. Yan, Stretchable freezing-tolerant triboelectric nanogenerator and strain sensor based on transparent, long-term stable, and highly conductive gelatin-based organohydrogel, Nano Energy. 95 (2022) 106967. https://doi.org/10.1016/J.NANOEN.2022.106967.